ELSEVIER

International Journal of Solids and Structures 41 (2004) 4989–5001

INTERNATIONAL JOURNAL OF SOLIDS and STRUCTURES

www.elsevier.com/locate/ijsolstr

Postbuckling and vibration of linearly elastic and softening columns under self-weight

L.N. Virgin [a,*], R.H. Plaut [b]

[a] *Department of Mechanical Engineering and Materials Science, Duke University, Duke Box 90300, Durham, NC 27708-0300, USA*
[b] *Charles E. Via, Jr. Department of Civil and Environmental Engineering, Virginia Polytechnic Institute and State University, Blacksburg, VA 24061-0105, USA*

Received 16 March 2004; received in revised form 16 March 2004
Available online 25 May 2004

Abstract

The critical height for buckling of a linearly elastic cantilevered column due to its self-weight was determined by Greenhill in 1881. Postbuckling behavior also has been studied, often assuming that the column is an elastica (inextensible, with its bending moment proportional to its curvature). The bifurcation point at the critical height is supercritical, so that the postbuckling path is stable as the height increases past its critical value. Subcritical bifurcation may occur if the column is nonlinearly elastic with a softening behavior. This results in a sudden jump from the straight vertical configuration to a severely-drooped shape. The governing equation is solved numerically with the use of a shooting method to obtain the equilibrium paths. Also, small vibrations about the straight and postbuckled equilibrium states are examined, and vibration frequencies (and hence stability properties) are obtained. An initial curvature of the column is included in the analysis. Experiments are conducted to verify the results qualitatively for linearly elastic and softening materials.

Keywords: Buckling; Vibration; Columns; Self-weight; Elastica; Softening

1. Introduction

In a classic paper, Greenhill (1881) considered a linearly elastic, uniform, cantilevered column subjected only to its self-weight. The linear equilibrium equation has a nonconstant coefficient. Greenhill obtained a solution in terms of Bessel functions and found the value of the critical height.

Large deflections for this problem have been treated in a number of papers, including Frisch-Fay (1961), Denman and Schmidt (1970), Schmidt and DaDeppo (1970), Wang (1971, 1986), Hsu and Hwang (1988), and Fraser and Champneys (2001) for uniform columns, and Stuart (2001) for a tapered column. The columns were assumed to be linearly elastic, with the curvature proportional to the bending moment. If the

* Corresponding author. Tel.: +1-919-660-5342; fax: +1-919-660-8963.
E-mail address: 1.virgin@duke.edu (L.N. Virgin).

0020-7683/$ - see front matter © 2004 Elsevier Ltd. All rights reserved.
doi:10.1016/j.ijsolstr.2004.03.023

height is plotted versus a displacement measure, the bifurcation at the critical height is supercritical. Therefore the column exhibits a smooth transition from the vertical configuration to stable drooped states, and the amount of droop increases continuously as the height of the column is increased.

Acheson (1997), Fraser and Champneys (2001), and Mullin et al. (2004) described experiments involving a curtain wire. It has an inner core consisting of a tightly-wound spring, covered by a plastic coating. This wire exhibits subcritical bifurcation. When the critical height is reached, the vertical wire suddenly jumps to a severely-drooped configuration. As explained by Fraser and Champneys (2001), this occurs because of the softening behavior of the wire when subjected to bending.

Inextensible columns with softening behavior are considered here. The curvature is assumed to be a cubic function of the bending moment and models the relationship for the curtain wire (a quintic function is used in one case). Linearly elastic behavior is a special case, leading to the standard elastica formulation. An initial deflection with constant curvature is included. Equilibrium paths are determined numerically using a shooting method. Small vibrations about equilibrium states are also investigated, and vibration frequencies are computed.

In Section 2, a linear analysis is carried out. Nonlinear equilibrium paths are examined in Section 3, and examples of supercritical and subcritical bifurcation are presented. Fundamental frequencies for vibrations about the equilibrium states are plotted. Experimental work is described in Section 4, using a linearly elastic fiber and a lexan rod, and the softening curtain wire mentioned above. Concluding remarks are given in Section 5. A similar type of investigation for a vertical half-loop under self-weight is presented in Plaut and Virgin (2004).

Some further related references can be mentioned. Wang (1996) analyzed the postbuckling of a cantilevered column with a softening behavior, subjected to a vertical load at its tip. Additional recent papers involving self-weight buckling include El Naschie and Hussein (2000), Li (2000, 2001), Teng and Yao (2000), and Lim and Ma (2003).

2. Small displacements

Consider the column shown in Fig. 1. It has height H, constant bending stiffness EI, and constant weight W per unit length. The equilibrium equation is

$$\mathrm{EI}Y''''(X) + W\left[(H-X)Y'(X)\right]' = 0. \tag{1}$$

To put the analysis in nondimensional terms, define

$$a = \left(\frac{\mathrm{EI}}{W}\right)^{1/3}, \quad x = \frac{X}{a}, \quad y = \frac{Y}{a}, \quad h = \frac{H}{a}. \tag{2}$$

(The lengths are not nondimensionalized by H, since the height is the parameter of interest.) This leads to the following equation:

$$y''''(x) + [(h-x)y'(x)]' = 0. \tag{3}$$

The boundary conditions are $y(0) = y'(0) = y''(h) = y'''(h) = 0$. The critical nondimensional height is $h_{\mathrm{cr}} = 1.986$ (Timoshenko and Gere, 1961; Wang, 1986).

Approximate values of the critical height can be obtained with the use of the Rayleigh–Ritz method (Marion and Thornton, 1988; Schmidt, 1998). The potential energy U is given by

$$U = \frac{1}{2}\int_0^h (y'')^2\,\mathrm{d}x - \frac{1}{2}\int_0^h (h-x)(y')^2\,\mathrm{d}x. \tag{4}$$

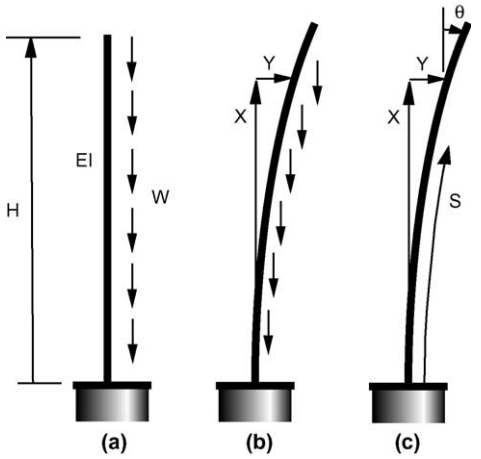

Fig. 1. Geometry of column subjected to self-weight.

Making U stationary for the kinematically admissible function $y(x) = a_1 x^b$, where $b > 1$ leads to the approximate critical height $h_{cr} = 2.289$ if $b = 2$, and the value $h_{cr} = 2.143$ for the minimizing choice $b = 1.747$. If $y(x) = a_1[1 - \cos(bx/h)]$, one obtains $h_{cr} = 2.025$ for $b = \pi/2$ (corresponding to the buckling mode for a cantilever with axial end load, as used in Virgin (1987)), and $h_{cr} = 2.003$ for the optimal value $b = 1.829$. Finally, the two-term approximation $y(x) = a_1 x^2 + a_2 x^3$ furnishes the excellent approximation $h_{cr} = 1.991$.

3. Large displacements

3.1. Formulation

Consider motion of the column and let T denote time. If the slope of the column is not small, the analysis is carried out in terms of the arc length S and the tangential angle $\theta(S, T)$ shown in Fig. 1(c), as well as the coordinates $X(S, T)$ and $Y(S, T)$. The bending moment is $M(S, T)$, the cross-sectional forces are $P(S, T)$ in the X direction and $Q(S, T)$ in the $-Y$ direction on a positive face, and the initial angle is $\theta_0(S)$ if the column is imperfect and has an initial displacement.

A nonlinear moment–curvature relationship is assumed with the form

$$\mathrm{EI}\left(\frac{\partial\theta}{\partial S} - \frac{\mathrm{d}\theta_0}{\mathrm{d}S}\right) = M\left[1 + c\left(\frac{Ma}{\mathrm{EI}}\right)^r\right], \tag{5}$$

where $c = 0$ for the usual linearly elastic elastica, and c and r are positive for softening behavior. Examples of this relationship in nondimensional terms ($m = Ma/\mathrm{EI}, s = S/a$) with $r = 2$ and $c = 4$ or 8 are plotted in Fig. 2, along with $c = 0$. The case $r = 2$ and $c = 4$ gives a good approximation to the behavior of the curtain wire used in Acheson (1997), Fraser and Champneys (2001), and Mullin et al. (2004), and in some of the experiments to be described in Section 4. This was determined by clamping different lengths of the curtain wire to form a horizontal cantilever, measuring the downward tip displacement caused by self-weight, and comparing the data to numerical results of a nonlinear beam analysis using (5) with various combinations of r and c.

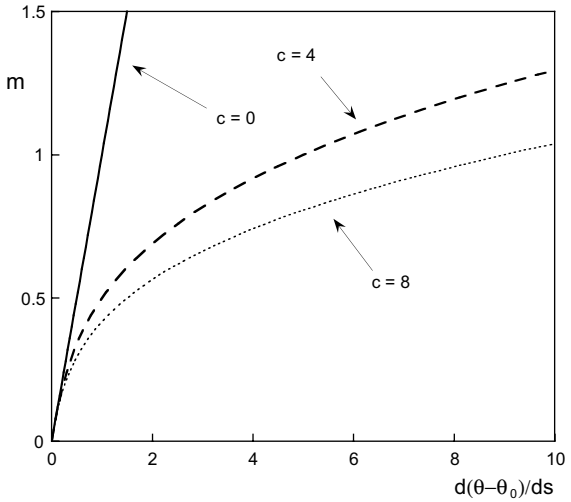

Fig. 2. Nondimensional moment–curvature relation with $r = 2$ and $c = 0, 4, 8$.

From geometry and equilibrium including inertia loads, and neglecting longitudinal and rotary inertias, the governing equations are

$$\begin{aligned}
&\frac{\partial X}{\partial S} = \cos\theta,\\
&\frac{\partial Y}{\partial S} = \sin\theta,\\
&\frac{\partial M}{\partial S} = P\sin\theta + Q\cos\theta,\\
&\frac{\partial P}{\partial S} = W + \frac{W}{g}\frac{\partial^2 X}{\partial T^2},\\
&\frac{\partial Q}{\partial S} = -\frac{W}{g}\frac{\partial^2 Y}{\partial T^2},
\end{aligned} \tag{6}$$

(where g is gravitational acceleration), along with the constitutive law (5). The quantities X, Y, θ, M, P, and Q are written in terms of an equilibrium component and a dynamic component involving a vibration mode with frequency ω, as follows:

$$\begin{aligned}
&X(S,T) = X_e(S) + X_d(S)\sin\omega T,\\
&Y(S,T) = Y_e(S) + Y_d(S)\sin\omega T,\\
&\theta(S,T) = \theta_e(S) + \theta_d(S)\sin\omega T,\\
&M(S,T) = M_e(S) + M_d(S)\sin\omega T,\\
&P(S,T) = -(H-S)W + P_d(S)\sin\omega T,\\
&Q(S,T) = Q_d(S)\sin\omega T.
\end{aligned} \tag{7}$$

($P = -(H-S)W$ and $Q = 0$ for equilibrium states.) These quantities are substituted into (5) and (6), and the nonlinear dynamic terms are neglected. Then the equations are put in nondimensional form using the

definitions of x, y, and h in (2), as well as $s = S/a, m = Ma/(\mathrm{EI}), p = Pa^2/(\mathrm{EI}), q = Qa^2/(\mathrm{EI}), \kappa = \mathrm{d}\theta_0/\mathrm{d}s, t = T\sqrt{g/a}$, and $\Omega = \omega\sqrt{a/g}$, where κ is the nondimensional initial curvature and will be constant in the numerical examples.

The equations governing equilibrium are obtained from the terms not involving $\sin \Omega t$, and are given by

$$\begin{aligned} x_e' &= \cos\theta_e, \\ y_e' &= \sin\theta_e, \\ \theta_e' &= m_e + c m_e^{r+1} + \kappa, \\ m_e' &= -(h-s)\sin\theta_e, \end{aligned} \tag{8}$$

where primes ($'$) denote differentiation with respect to s. The boundary conditions at $s = 0$ are $x_e = y_e = \theta_e = 0$, while $m_e = 0$ at $s = h$.

The equations governing small vibrations about an equilibrium state are

$$\begin{aligned} x_d' &= -\theta_d \sin\theta_e, \\ y_d' &= \theta_d \cos\theta_e, \\ \theta_d' &= m_d + (r+1) c m_e^r m_d, \\ m_d' &= [q_d - (h-s)\theta_d]\cos\theta_e + p_d \sin\theta_e, \\ p_d' &= -\Omega^2 x_d \\ q_d' &= \Omega^2 y_d. \end{aligned} \tag{9}$$

At $s = 0, x_d = y_d = \theta_d = 0$, and at $s = h, m_d = p_d = q_d = 0$.

3.2. Numerical results

Numerical solutions are obtained using a shooting method with the subroutines NDSolve and FindRoot in Mathematica (Wolfram, 1991). To obtain nontrivial equilibrium states using (8), values of κ, c, r, and $m_e(0)$ are specified, and h is varied until $m_e(h) = 0$ with sufficient accuracy. The value of $m_e(0)$ is changed to determine the equilibrium path.

Results for the linearly elastic case (the elastica) are shown in Fig. 3(a), where the height h is plotted versus the lateral tip deflection $y(h)$. If the column has no initial curvature ($\kappa = 0$), there is a trivial solution $y_e(x) = 0$. The first bifurcation point occurs at the critical height $h_{\mathrm{cr}} = 1.986$, and the trivial solution is unstable for larger values of h. The bifurcation point is supercritical (i.e., stable-symmetric), and the column smoothly begins to droop as the height is increased past its critical value. Equilibrium paths are also

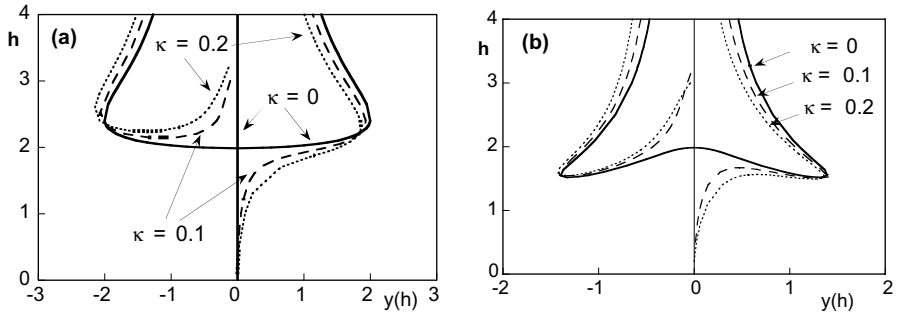

Fig. 3. Equilibrium paths for (a) linearly elastic column ($c = 0$), (b) softening column with $r = 2$ and $c = 4$.

depicted for the initial curvatures $\kappa = 0.1$ and 0.2. The primary imperfect paths emanating from $h = 0$ consist of stable equilibrium states. The secondary imperfect paths are stable to the left of their minima. The portions to the right of the minima are unstable and are cut off in Fig. 3(a); they continue to rise and approach a postbuckled perfect path associated with the second bifurcation point ($h = 3.823$). A perspective of a linearly elastic drooped configuration is drawn in Fig. 4(a). For drooped shapes, h should be interpreted physically as the nondimensional length of the column, rather than the height.

Results are presented in Fig. 3(b) for a nonlinearly elastic (softening) column with $r = 2$ and $c = 4$ in the moment–curvature relationship (5). The bifurcation is subcritical. For the perfect case ($\kappa = 0$), when the height h reaches the critical value 1.986 the configuration jumps from the straight vertical shape to a severely-drooped shape with its tip below the base at $(x_e, y_e) = (-1.29, 1.11)$ and tip rotation $\theta_e = 2.71$. If the initial curvature is $\kappa = 0.1$, the equilibrium path has a limit (turning) point at $h = 1.671$ with tip values $(x_e, y_e, \theta_e) = (1.59, 0.47, 0.45)$, and the column then suddenly moves to a drooped configuration with $(x_e, y_e, \theta_e) = (-0.59, 1.31, 2.37)$ at its tip. Similarly, if $\kappa = 0.2$, the limit point occurs at $h = 1.564$ with $(x_e, y_e, \theta_e) = (1.39, 0.66, 0.69)$ at the tip, and the column then suddenly moves to a state with $(x_e, y_e, \theta_e) = (-0.19, 1.35, 2.14)$ at its tip. The unstable parts of the secondary paths are cut off at $y(h) = 0$.

Plotted in Fig. 4(b) is a sequence of events as the length of a slightly imperfect, drooped softening column is gradually reduced. Starting from the heavily postbuckled point A, the length is reduced with the tip of the column passing through points B, C, and D, at which point the local minimum of the equilibrium path is reached, causing the column to dynamically spring to its (almost) upright position. These minima are near $h = 1.5$ in Fig. 3(b). Computations also were carried out for the case $r = 2$ and $c = 8$. The equilibrium paths are similar to those in Fig. 3(b). The limit point occurs at $h = 1.612$ if $\kappa = 0.1$, and at $h = 1.494$ if $\kappa = 0.2$.

The equilibrium paths can also be plotted with the height as a function of the base moment, and representative plots for the linearly elastic and softening columns are shown in Fig. 5(a) and (b), respectively.

For the column with no initial curvature ($\kappa = 0$), it is of interest to know if the bifurcation point is supercritical, as in Figs. 3(a) and 5(a), or subcritical, as in Figs. 3(b) and 5(b). Equilibrium paths of height versus base moment are plotted in Fig. 6(a) for $r = 2$ and in Fig. 6(b) for $r = 4$. For $r = 2$, the bifurcation is supercritical if $c < 0.2$. Hence the curve for $c = 0.1$ rises as the nontrivial path leaves the bifurcation point, but the curves for $c = 0.5$ and 1.0 initially fall. For $r = 4$, all curves in Fig. 6(b) initially rise. However, this local behavior does not imply here that the curves continue to rise. The postbuckling curves in Fig. 6(b)

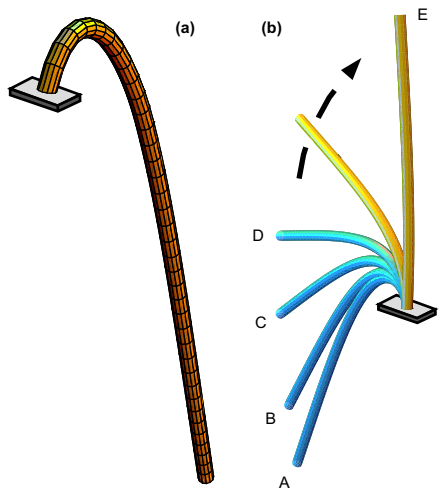

Fig. 4. (a) A stable drooped configuration for the linearly elastic column, (b) a sequence of states for the softening column.

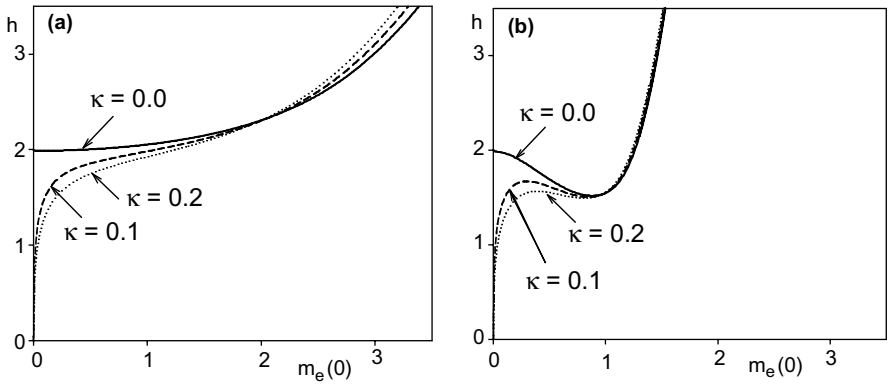

Fig. 5. Height versus base moment: (a) linearly elastic, (b) softening ($r = 2, c = 4$).

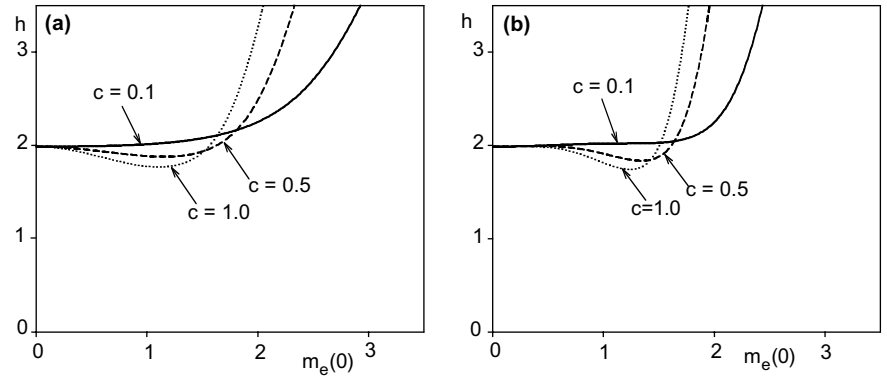

Fig. 6. Height versus base moment, $\kappa = 0$: (a) $r = 2$, (b) $r = 4$.

exhibit a limit (maximum) point, then fall to a local minimum point, and then rise again. For $c = 0.5$ and 1.0, this behavior is significant. Even though the bifurcation point is stable-symmetric, if there were a sufficiently small imperfection, the equilibrium path would exhibit a limit point at a lower height than the critical one, which is behavior normally associated with an unstable bifurcation point.

Fig. 7 shows the equilibrium shapes for the linearly elastic column ($\kappa = 0$) in which each position corresponds to an incremental increase in base moment starting from just beyond the critical point.

Fundamental vibration frequencies are plotted in Figs. 8 and 9. The ordinate is the height h and the abscissa is Ω^2, the square of the frequency for small vibrations about the equilibrium state. Negative values of Ω^2 are associated with unstable equilibrium states and with motions that grow exponentially (so Ω is then not a vibration frequency). In the application of the shooting method to solve Eq. (9) numerically, the equilibrium state is known. The vibration amplitude is arbitrary, so $m_d(0)$, for example, is given a value, and $p_d(0), q_d(0)$, and Ω^2 are varied until $m_d(h) = p_d(h) = q_d(h) = 0$ with sufficient accuracy.

The linearly elastic case ($c = 0$) is considered in Fig. 8. For the perfect column ($\kappa = 0$), the solid curve corresponds to vibrations about the straight configuration, which is stable for $h \leqslant 1.986$. The fundamental frequency is zero at the critical height. The curve is convex toward the origin, unlike typical characteristic curves in which a loading parameter (rather than the height) is plotted versus the frequency squared (Huseyin, 1978). Frequencies for vibrations about the stable postbuckled equilibrium path for the perfect

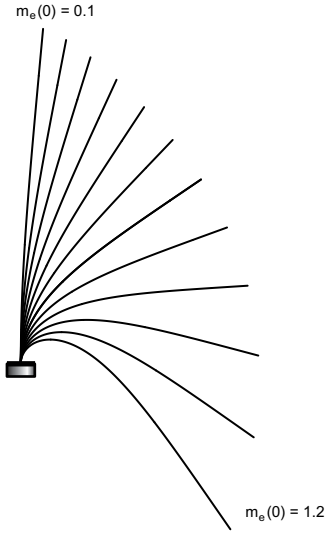

Fig. 7. Deflected shapes as the base moment is incrementally changed ($\kappa = 0$).

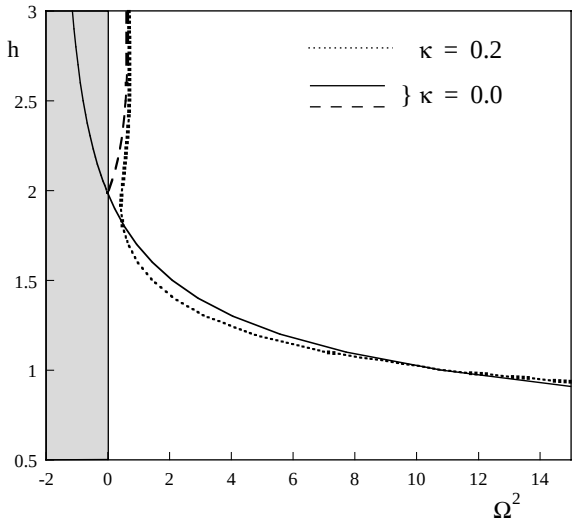

Fig. 8. Height versus square of fundamental frequency for linearly elastic column.

column are plotted as the dashed curve. For the imperfect case $\kappa = 0.2$, frequencies are shown as the dotted curve. The equilibrium states are stable. As the height is increased, the fundamental frequency decreases till the height h is close to its critical value for the perfect column, and then the frequency increases.

Results are presented in Fig. 9 for the softening column with $r = 2$ and $c = 4$. For the perfect case, frequencies for small vibrations about the straight configuration are not affected by the nonlinearity in the moment–curvature relationship, and hence the solid curve is the same as in Fig. 8. For the bifurcating path, the equilibrium states in Fig. 3(b) are unstable from the bifurcation point to the minimum point. Hence the corresponding squares of the frequencies on the dashed curve in Fig. 9 are negative from $h = 1.986$ till

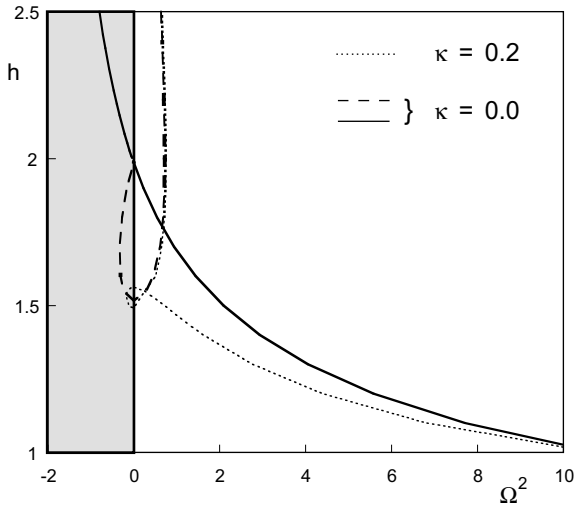

Fig. 9. Height versus square of fundamental frequency for softening column ($r = 2, c = 4$).

$h = 1.517$ (where $\Omega^2 = 0$ again), and then become positive along the equilibrium path. For the imperfect case $\kappa = 0.2$, the dotted curve has a local maximum at the critical height $h = 1.564$. The values of the frequency squared are negative when the equilibrium path is between the limit point and the turning point at $h = 1.492$ in Fig. 3(b), and then are positive and are almost the same as those for the perfect column.

4. Experiments

A number of simple experiments were conducted on slender struts which could be extended to a sufficient vertical length such that self-buckling was induced. For the linearly elastic case, two columns were tested. First, equilibrium paths and natural frequencies were determined using an axisymmetric fiber-optic filament. The fiber was placed in an upright position and the length was incrementally increased. Fig. 10(a) shows a typical equilibrium path which suggests buckling between $H = 15$ and 20 cm. In this case an estimate of the flexural rigidity was obtained from the droop of a horizontal fiber cantilever, and using the theoretical critical length, $1.986(\mathrm{EI}/W)^{1/3}$, resulted in an estimate very close to 20 cm, which is close to the height at the minimum value of the fundamental frequency, also shown in Fig. 10(a). The linearly elastic column clearly exhibits a supercritical bifurcation with a continuous deflected configuration throughout the change in length.

Second, a flat, slender strip of lexan was used to measure some more natural frequencies in which the geometry of the cross section ensured unambiguous motion in a plane. The free end of the strut was subjected to a small perturbation and subsequent oscillations were monitored using a laser vibrometer. The fundamental frequency content was then extracted, with the results shown in Fig. 10(b). The reduction in the lowest natural frequency can clearly be seen as buckling is approached (the theoretical critical length is approximately 110 cm in this case), together with an increase in the postbuckling frequencies. The form of the length–frequency relation follows the theoretical curves depicted in Fig. 8 quite closely. Also, the inevitable presence of a little damping has a minor effect on the frequencies, but this is not considered in the analysis in this paper.

A softening cable (the curtain wire mentioned in Section 1) was also subjected to some simple experiments. A photograph of the cable in a postbuckled (drooped) equilibrium configuration is shown in Fig. 11.

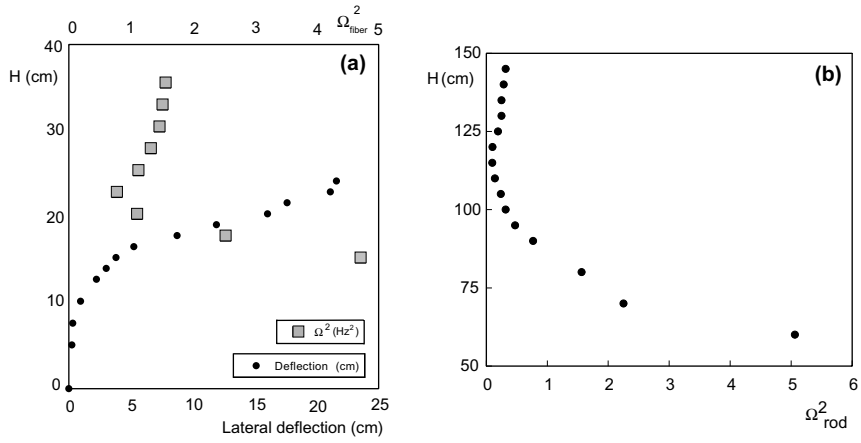

Fig. 10. (a) Tip deflection and fundamental frequency for fiber, (b) fundamental frequency for lexan rod.

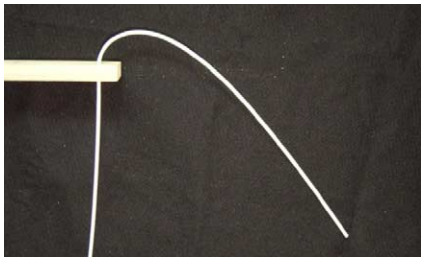

Fig. 11. A photograph of the softening cable column in a postcritical equilibrium configuration.

Again, the strut (with a circular cross section consisting of a plastic-coated, tight steel coil) was mounted vertically with a clamped boundary condition at the base. The static equilibrium deflections together with the frequencies of small-amplitude vibrations were measured. Fig. 12(a) shows the equilibrium path as a relation between the length of the cable and the horizontal deflection at the tip. The sudden jump at criticality is evident, when the length is a little over 40 cm (triangles). Since the subcritical bifurcation is associated with imperfection sensitivity, the critical length for the trivial equilibrium position may change quite drastically due to small initial imperfections. The cable is not quite perfectly straight in its unstressed configuration. The sensitivity of this system is highlighted by a second set of measurements taken from nominally the same system (in fact, using the other end of the cable sample), for which the critical length (at the limit point) was found to be about 47 cm (circles). Next, the length of the severely-drooped cable was reduced. In both cases, the critical length associated with the droop just prior to a dynamic return to the upright position (leftward-pointing arrow in Fig. 12(a)) was found to be about 37 cm, i.e., at the other end of the hysteresis cycle. In some ways this is not so surprising since that critical point (the minimum point in Fig. 3(b)) is associated with a regular limit point (i.e., not a perturbed subcritical bifurcation) and hence is not imperfection sensitive.

Some fundamental natural frequencies are shown in Fig. 12(b). These were taken from the original test (corresponding to the triangles in Fig. 12(a)) and clearly show the decay towards zero. They have essentially the same form as for the linearly elastic case until buckling occurs (circles), as mentioned earlier. One practical difference is that in the subcritical case it becomes very difficult to generate finite vibrations, due to

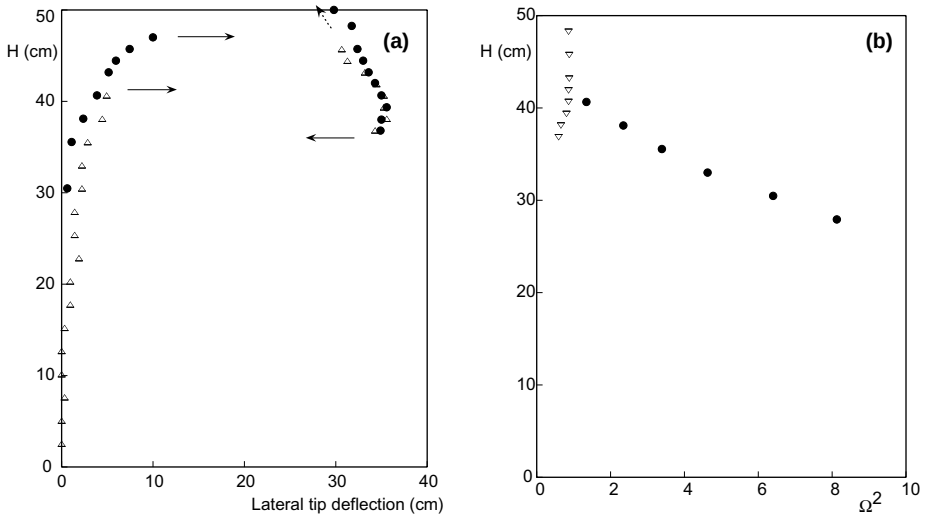

Fig. 12. The relation between cable length, lateral deflection, and frequencies of small oscillations.

the shrinking basin of attraction as criticality is approached. After the finite jump at the critical limit point, the system restabilizes onto the stable remote postbuckled (drooped) equilibrium path and natural frequencies of small oscillations begin to increase as the droop increases (triangles). The hysteresis is again illustrated by subsequently reducing the cable length and observing real frequencies till the cable snaps back up to its vertical position (which occurs for a shorter length than the initial loss of stability). As for the fiber and the lexan rod, this sequence of events in the experimental frequency–load relation shows a good qualitative agreement with the theoretical results.

5. Concluding remarks

Inextensible cantilevered columns with linearly elastic or softening behavior have been considered. The columns were only subjected to their self-weight, and were either perfect or were imperfect with a constant initial curvature. Equilibrium configurations and small vibrations about those states were investigated. Both numerical and experimental results were presented.

If the column is linearly elastic, it is not imperfection sensitive. When it is perfect and its height is increased, it transitions smoothly from its vertical configuration to a postbuckled (drooped) shape after the critical height ($h = 1.986$) is reached. When it has an initial curvature, its shape changes smoothly as its length is increased.

If the column has the softening moment–curvature relation given by (5) with $c = 4$ and $r = 2$ (Fig. 2), the bifurcation at the critical height is subcritical (unstable-symmetric) instead of supercritical (stable-symmetric), and the column is imperfection sensitive. For the perfect case, the column jumps to a severely-drooped configuration when the critical height ($h = 1.986$) is attained. If the column has a small initial curvature, a jump occurs when the height reaches a lower value. This softening model is based on the behavior of a curtain wire consisting of a tightly-wound steel spring covered by a plastic coating. Its buckling behavior under self-weight is hence quite different from that of a typical isotropic column, even though its critical height in nondimensional terms is the same.

An interesting type of behavior was shown in Fig. 6(b). If the coefficient of the nonlinear softening term is not sufficiently large, the bifurcation is stable-symmetric and the postbuckling curve rises initially.

However, it then may fall to a minimum value significantly lower than the bifurcation value. Thus a disturbance to the perfectly-straight vertical column may cause it to jump to a stable drooped state before the critical height is reached, and with small imperfections, the column acts like an imperfection sensitive system having an unstable bifurcation point.

Small vibrations about the prebuckled and postbuckled equilibrium states were examined. The fundamental frequency is zero at the bifurcation and limit (turning) points on the equilibrium paths. Therefore these critical points can sometimes be predicted by extrapolating frequency data at various levels of load or height before instability occurs (Plaut and Virgin, 1990; Virgin and Plaut, 2002).

Some simple experiments verified the main features of the equilibrium and dynamic behavior for both the linearly elastic and softening columns.

A planar half-loop, which lies above two vertical clamped supports and is subjected to self-weight, is analyzed in a companion paper (Plaut and Virgin, 2004). When its length is increased, it exhibits some similarities in stability and vibration behavior to the column considered here.

Acknowledgements

The authors are grateful to Stacia S. Keller and Meeok Kim at Virginia Tech for carrying out some of the computations, and to R. Ben Davis at Duke University for assisting with the experiments. They also acknowledge helpful comments from the reviewers.

References

Acheson, D., 1997. From Calculus to Chaos: an Introduction to Dynamics. Oxford University Press, Oxford.

Denman, H.H., Schmidt, R., 1970. An approximate method of analysis of large deflections.. Z. Angew. Math. Phys. 21, 412–421.

El Naschie, M.S., Hussein, A., 2000. On the eigenvalue of nuclear reaction and self-weight buckling. Chaos, Solitons & Fractals 11, 815–818.

Fraser, W.B., Champneys, A.R., 2001. The 'Indian rope trick' for a parametrically excited flexible rod: nonlinear and subharmonic analysis. Proc. R. Soc. Lond. A 458, 1353–1373.

Frisch-Fay, R., 1961. The analysis of a vertical and a horizontal cantilever under a uniformly distributed load. J. Franklin Inst. 271, 192–199.

Greenhill, A.G., 1881. Determination of the greatest height consistent with stability that a vertical pole or mast can be made, and of the greatest height to which a tree of given proportions can grow. Proc. Cambr. Phil. Soc. 4, 65–73.

Hsu, S.-B., Hwang, S.-F., 1988. Analysis of large deformation of a heavy cantilever. SIAM J. Math. Anal. 19, 854–866.

Huseyin, K., 1978. Vibrations and Stability of Multiple Parameter Systems. Noordhoff, Alphen aan den Rijn, The Netherlands.

Li, Q.S., 2000. Exact solutions for buckling of non-uniform columns under axial concentrated and distributed loading. Eur. J. Mech. A 20, 485–500.

Li, Q.S., 2001. Analytical solutions for buckling of multi-step columns with arbitrary distribution of flexural stiffness or axial distributed loading. Int. J. Mech. Sci. 43, 349–366.

Lim, C.W., Ma, Y.F., 2003. Computational *p*-element method on the effects of thickness and length on self-weight buckling of thin cylindrical shells via various shell theories. Comp. Mech. 31, 400–408.

Marion, J.B., Thornton, S.T., 1988. In: Classical Dynamics of Particles & Systems, third ed. Harcourt Brace Jovanovich, Fort Worth, p. 461.

Mullin, T., Champneys, A., Fraser, W.G., Galan, J., Acheson, D., 2004. The 'Indian rod trick' via parametric excitation. Proc. R. Soc. Lond. A (submitted).

Plaut, R.H., Virgin, L.N., 1990. Use of frequency data to predict buckling. J. Sound Vib. 116, 2330–2335.

Plaut, R.H., Virgin, L.N., 2004. Three-dimensional postbuckling and vibration of vertical half-loop under self-weight (in press).

Schmidt, R., 1998. Modifying Rayleigh's own method for estimating buckling loads and other eigenvalues. Indus. Math. 48, 101–105.

Schmidt, R., DaDeppo, D.A., 1970. Large deflection of heavy cantilever beams and columns. Quart. Appl. Math. 28, 441–444.

Stuart, C.A., 2001. Buckling of a heavy tapered rod. J. Math. Pures Appl. 80, 281–337.

Teng, J.G, Yao, J., 2000. Self-weight buckling of FRP tubes filled with wet concrete. Thin-Walled Struct. 38, 337–353.

Timoshenko, S.P., Gere, J.M., 1961. In: Theory of Elastic Stability, second ed. McGraw-Hill, New York, pp. 101–103.
Virgin, L.N., 1987. Free vibrations of imperfect cantilever bars under self-weight loading. J. Mech. Engng. Sci. 201, 345–347.
Virgin, L.N., Plaut, R.H., 2002. Use of frequency data to predict secondary bifurcation. J. Sound Vib. 251, 919–926.
Wang, C.Y., 1986. A critical review of the heavy elastica. Int. J. Mech. Sci. 28, 549–559.
Wang, C.Y., 1996. Global buckling load of a nonlinearly elastic bar. Acta Mech. 119, 229–234.
Wang, T.M., 1971. Postbuckling of column under distributed axial load. J. Engng. Mech. 97, 1323–1327.
Wolfram, S., 1991. Mathematica: a System for Doing Mathematics by Computer. Addison-Wesley, Reading, MA.